



## Variations of regional background peroxyacetyl nitrate in marine boundary layer over Baengyeong Island, South Korea

Gangwoong Lee<sup>a,\*</sup>, Hee-Soon Choi<sup>a</sup>, Taehyoung Lee<sup>b</sup>, Jinsu Choi<sup>c</sup>, Jin Su Park<sup>c</sup>, Joon Young Ahn<sup>c</sup>

<sup>a</sup> Department of Environmental Science, Hankuk University of Foreign Studies, Yongin, Republic of Korea

<sup>b</sup> Department of Atmospheric Science, Colorado State University, Fort Collins, USA

<sup>c</sup> Climate & Air Quality Research Department, National Institute of Environmental Research, Incheon, Republic of Korea

### H I G H L I G H T S

- ▶ PAN in autumn was the highest due to frequent transports from source regions.
- ▶ The maximum levels of PAN were observed at airs originated from mid-altitudes.
- ▶ The marine boundary layer acted as an overall sink for PAN.
- ▶ In-situ PAN production within boundary airs was apparent under some conditions.
- ▶ PAN in this study was two times higher than previous studies in the Yellow Sea.

### A R T I C L E I N F O

#### Article history:

Received 13 February 2012

Received in revised form

30 July 2012

Accepted 31 July 2012

#### Keywords:

PAN

Baengyeong Island

Long-range transport

Ozone

Photochemistry

Boundary layer

### A B S T R A C T

Concurrent two-week measurements of peroxyacetyl nitrate (PAN), other photochemically reactive species (including O<sub>3</sub>, CO, NO<sub>2</sub>, and volatile organic compounds), and aerosols (water-soluble ionic species, organic and elemental carbon, and trace metals) were made at an atmospheric monitoring station on Baengyeong Island in the summer and autumn of 2010 and winter and spring of 2011. PAN mixing ratios ranged from the below the detection limit of 0.01–2.47 ppbv, with a median of 0.04, 0.58, 0.32, 0.17 ppbv during the summer, autumn, winter; and spring, respectively. Although the photochemical ages determined from the PAN/NO<sub>x</sub> ratios indicated that the measurement site was situated under a relatively clean marine boundary layer, significant and abrupt increases in PAN were frequently observed due to transport from nearby land masses, mainly China and South Korea. The vertical trend of PAN with a mid-altitude maximum observed in this study is consistent with previous aircraft campaigns near the site. However, the PAN concentration recorded in this study was about two times higher than those of previous studies at remote marine surface sites in the southern Yellow Sea. In most cases, the marine boundary layer acted as an overall sink for PAN. However, we found that in-situ photochemical production of insoluble PAN also contributes to maintaining high-PAN mixing ratios in the boundary layer over the Yellow Sea and plays a role in the regional transport of reactive nitrogen species.

© 2012 Elsevier Ltd. All rights reserved.

### 1. Introduction

PAN, like O<sub>3</sub>, is a secondary pollutant that is photochemically produced from precursor gases such as nitrogen oxides (NO<sub>x</sub>) and volatile organic compounds (VOCs). Although PAN and O<sub>3</sub> share common precursors and are often considerably correlated with each other, PAN is known as a better indicator of photochemical air

pollution because it originates solely from photochemical reactions, whereas O<sub>3</sub> is often significantly influenced by other sources such as stratospheric intrusion (Nielsen et al., 1981). Furthermore, PAN has long been considered an important pollutant as it is likely to lead to widespread acid deposition, with harmful effects on vegetation (Cape, 2003). Due to its high production rate near NO<sub>x</sub> and VOCs source regions, PAN mixing ratios have been measured in excess of a few ppbv in urban areas. PAN is also ubiquitous at levels of a few pptv in remote marine environments, although mixing ratios in Antarctica are often down to sub-pptv levels (Gallagher et al., 1990; Muller and Rudolph, 1992; Staudt et al., 2003; Mills et al., 2007).

\* Corresponding author.

E-mail address: [gwlee@hufs.ac.kr](mailto:gwlee@hufs.ac.kr) (G. Lee).

In East Asia, anthropogenic emissions are considered to be rapidly increasing and are predicted to increase further (Akimoto, 2003; Ohara et al., 2007). The apparent increasing trend in the  $O_3$  mixing ratio at background sites in Northeast Asia over the last two decades points to the considerable effect of increasing emissions from Asia. Furthermore, the increases in background  $O_3$  over Europe and North America cannot be solely explained by regional  $O_3$  precursor changes because anthropogenic  $O_3$  precursor emissions decreased in Europe and North America as consequence of strict air pollution legislation (Staehelin and Poberaj, 2007). Xu et al. (2008) observed long-term trends showing an increase in the daily  $O_3$  maximum at a regional background station in eastern China, which was attributed mainly to increasing  $NO_x$  concentrations. There are also numerous reports showing that pollutants from Asia are transported over the Pacific to North America (Singh et al., 2009; Reidmiller et al., 2009). Wild et al. (2004) showed that outflow from East Asia can affect the  $O_3$  concentration on a global scale. PAN transported away from source regions is the key reactive nitrogen species responsible for  $O_3$  formation in remote regions (Crutzen, 1979; Ridley et al., 1990; Hudman et al., 2004).

The lifetime of PAN after formation is highly sensitive to temperature: it is 5.36 years at  $-26\text{ }^\circ\text{C}$  but just 30 min at  $25\text{ }^\circ\text{C}$  (Zhang et al., 2011). Thus, the extent of long-range transport of PAN significantly varies with the time of day, season, path and altitude, and weather processes during transport. Near the source regions, the maximum PAN mixing ratios are observed during late spring and summer, when the photochemical production is the highest. In contrast, in remote areas, the maximum PAN mixing ratios are often found in winter time as a result of the increased stability of PAN at the lower temperatures (Gaffney and Marley, 1993; Rubio et al., 2007). The prevailing winds in Northeast Asia are greatly complicated by seasonal circulation patterns that overlap the mid-latitude westerly. Thus, pollution transport over this region is frequently subject to the influence of monsoon air flows, which represent the major seasonal changes in circulations affecting pollutant distribution (Sun et al., 2011). Although the Yellow Sea,

surrounded by China and the Korean Peninsula, is an ideal place to examine the long and medium-range transport of PAN and other photochemical pollutants, their concentrations have rarely been measured in a systematic manner in marine background atmospheres.

In order to assess the extent and identify the pathways of long-range transport of reactive nitrogen species, including the PAN, from East Asia, it is essential to know the key behaviors and conditions involved in PAN and  $O_3$  chemistry in the marine boundary layer near major source regions. Thus, the objectives of this study were to determine PAN mixing ratios in different seasons over the Yellow Sea and to investigate their variations according to transport effects, in-situ production, and loss within the boundary layer.

## 2. Experiment

Seasonal PAN measurements were conducted at an atmospheric supersite on Baengyeong Island, located in the far western part of Korea, in the Yellow Sea between China and Korea (Fig. 1). The measurement station ( $37^\circ 57' \text{ N}$ ,  $124^\circ 37' \text{ E}$ ) is located at the top of a hill in a mountainous area with an altitude of 150 m above sea level. The Korea National Institute of Environmental Research (NIER) established this atmospheric monitoring station to observe the regional background. The island has a population of about 4000 people who mainly reside on the eastern part. The influence of local emissions is practically confined to a narrow region because of the easterly wind and infrequent traffic on nearby roads.

Intensive seasonal field experiments were conducted in summer (August 2nd–14th, 2010), autumn (October 1st–16th, 2010), winter (January 14th–29th, 2011), and spring (March 28th–April 12th, 2011). PAN measurements were conducted in a room on the first floor of a station where 56 VOCs species were determined in-situ by an online gas chromatograph (GC) on an hourly basis. PAN mixing ratios were determined every 3 min by a fast chromatograph with luminol-based chemiluminescence

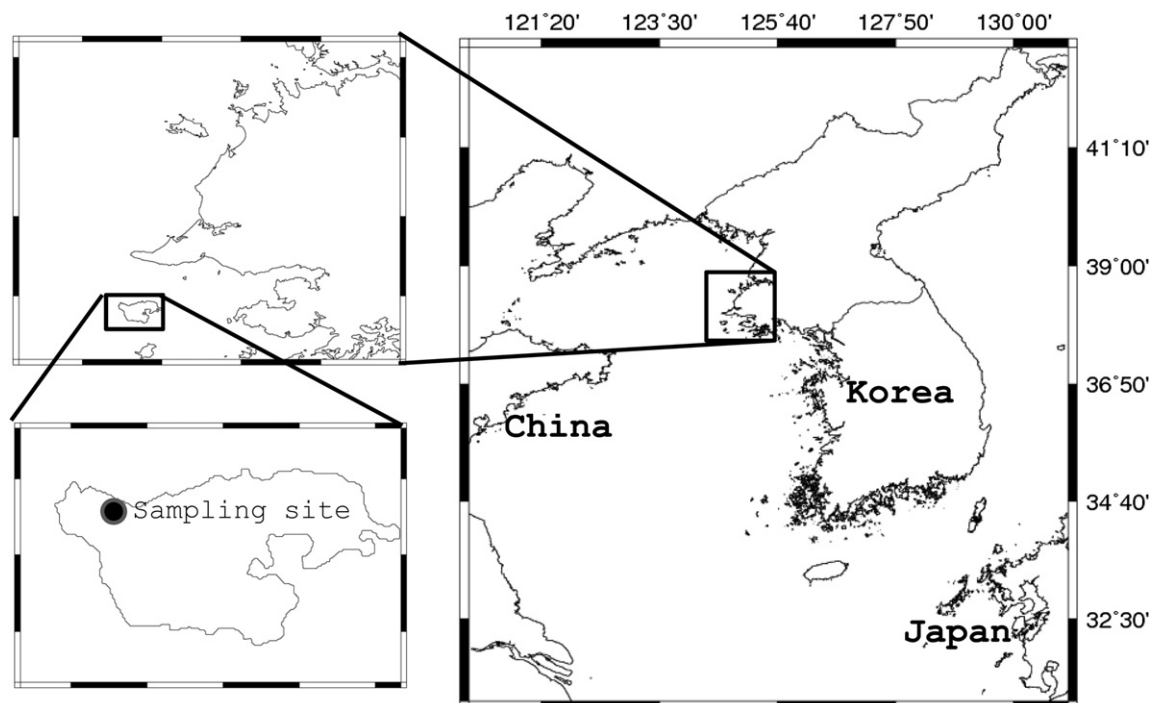


Fig. 1. Location of sampling site on Baengyeong Island in the Yellow Sea.

detection (Marley et al., 2004; Lee et al., 2008). Although a common glass inlet (1 inch diameter) and manifold were used to sample the air for VOCs and other gaseous compounds at the site, an independent perfluoroalkoxy line (1/4 inch) was used to directly sample the ambient air and thus reduce the length of the sample line to the PAN instrument. Air was continuously flushed at  $100 \text{ ml min}^{-1}$  to a  $2\text{-cm}^3$  Teflon loop attached to a six-port, two-position switching valve (Cheminert C22, Valco Instruments (Houston, TX, USA)) by a vacuum pump. The valve was cycled to injection/sampling positions by commands sent via an RS-232 serial port. PAN in the injected air samples was separated with  $\text{NO}_2$  and other chemiluminescence reacting species along a 10-m capillary GC column (DB-1, J&W Scientific, Folsom, CA, USA), and was introduced to a reaction cell connected to one end of the GC column. The PAN chemiluminescence signal, i.e., chromatogram peak, was detected by a gated photon counter (HC135-01, Hamamatsu, Bridgewater, NJ, USA) set at around 800 V and operated at room temperature. Photons from the PAN chemiluminescence reaction were counted by a PC through the RS-232 port. The whole process, including PAN peak identification and integration, was automated using a customized LabView (National Instruments, Austin, TX, U.S.A.) program with the serial data acquisition interface.

PAN calibration was carried out at the beginning and end of each experiment against liquid standards synthesized by nitration of peracetic acid in *n*-tridecane (Gaffney et al., 1984; Gregory et al., 1990). For this calibration, 1–5  $\mu\text{L}$  aliquots of the PAN/*n*-tridecane solution were injected through the injection port into a 5-L Tedlar bag filled with zero air (99.999%). After letting the air in the bag equilibrate for 2 min, it was connected to the sampling line and injected into the GC system. Immediately after being injected into the GC system, the air in the same bag was introduced to an  $\text{NO}_2$  chemiluminescence instrument (42C, Thermo Electron Corporation, Franklin, MA, USA) to read the PAN concentration in the form of  $\text{NO}_2$ . The above calibration procedure was completed in less than 5 min to minimize errors from the possible thermal decomposition of PAN (Kourtidis et al., 1993). As the nominal detection limit of  $\text{NO}_2$  for a commercial instrument is 1 ppbv, the calibrations were conducted at a range higher than 1 ppbv PAN. In comparison, the detection limit of PAN for our GC/Luminol system was estimated to be 0.01 ppbv, which was defined as three times the standard deviation of 7 signal noises. Based on the calibration, the response of the GC/Luminol system to PAN was linear and its precision and accuracy were estimated to be 5% and 16%, respectively. Nonetheless, the uncertainty was likely to be greater at concentrations below 1 ppbv.

A comprehensive set of gaseous and aerosol species was monitored routinely at the site by NIER. For gaseous species— $\text{O}_3$ ,  $\text{NO}_x$ , CO, and  $\text{SO}_2$ —and VOCs were measured on an hourly basis.  $\text{O}_3$  was sampled at 1-min intervals based on the UV absorption method (49C Thermo Electron Corporation, Franklin, MA, USA) and calibrated by an  $\text{O}_3$  transfer standard with a self-contained  $\text{O}_3$  generator.  $\text{NO}$ ,  $\text{NO}_2$ ,  $\text{NO}_x$ , and  $\text{NO}_y$  concentrations were measured every minute with two chemiluminescence instruments equipped with Mo converters (42C and 42CY, Thermo Electron Corporation, Franklin, MA, USA). The  $\text{NO}/\text{NO}_x$  and  $\text{NO}_y$  analyzer was calibrated in the range of 1–200 ppbv NO and propyl nitrate (RIGAS, Daejeon, South Korea) by diluting the NO standard (Deokyang Gas, Korea) using a dynamic calibrator (Thermo Electron Corporation, Franklin, MA, USA). CO was quantified every minute utilizing the gas filter correlation/non-dispersive infrared absorption spectroscopy method (48C, Thermo Electron Corporation, Franklin, MA, USA). The CO analyzer was standardized in the range of 0.5–2 ppmv every 2 weeks using CO standards (Deokyang Gas, Korea) with the same dynamic calibrator. Hourly VOCs were routinely quantified by two-column automated GC with two flame ionization

detectors (Varian, Walnut Creek, CA, USA) and a thermal desorption unit (UNITY, UK). One GC column was used to separate the more volatile organics and the other for the less volatile compounds. The detection limits for the two GCs were 0.5 ppbC propane and benzene, respectively.

The major chemical components (water-soluble ionic compositions and elemental carbon (EC)/organic carbon (OC)) of  $\text{PM}_{2.5}$  aerosols in were analyzed by online ion chromatography (URG 9000D, URG Corp., Chapel Hill, NC, U.S.A.) and a continuous EC/OC instrument (Model 4, Sunset Laboratory, Tigard, OR, U.S.A.). Meteorological parameters, including air temperature, relative humidity, wind direction, and wind speed, were also measured at a neighboring meteorological station operated by the Korea Meteorological Agency.

### 3. Results

#### 3.1. Time variations

As listed in Table 1, the overall mean PAN level (0.38 ppbv) at Baengyeong station was lower than in urban areas in northeast Asia, where it ranges from 0.8 to 1.4 ppbv (Lee et al., 2008; Zhang et al., 2011). However, only limited numbers of atmospheric PAN measurements at remote sites in East Asia are available for comparison. The PAN levels observed during this study were similar to the summertime average PAN of 0.44 ppbv at a background site at Mt Waliguan, China (Zhang et al., 2009) but higher than the values (0.01–0.2 ppbv) at remote islands near the Yellow Sea (Watanabe et al., 1998). The overall mean CO (269 ppbv) and  $\text{NO}_y$  (4.40 ppbv) at Baengyeong station were much higher than those in Mt Waliguan (149 and 1.41 ppbv, respectively). The low temperatures at the high altitudes on Mt Waliguan, and thus the increased stability of PAN, explain the relatively high PAN mixing ratios despite the low precursor availability. Pochanart et al. (2004) showed that air masses (regionally polluted continental air) impacted by large-scale East Asian anthropogenic emissions had typical CO levels higher than 200 ppbv, whereas the clean background values were only 167 ppbv. Thus, it is obvious that the air masses on Baengyeong Island are greatly influenced by the nearby anthropogenic sources from China and Korea.

From the hourly PAN variations (Fig. 2), we see large day-to-day variability in all seasons with maxima of 0.76, 2.57, 2.47, 1.01 ppbv for summer, autumn, winter, and spring, respectively. A few cases of episodic increased PAN for short periods were observed, especially in summer and winter. These periods were coincident with the arrival of fast moving air masses that had recently passed over populated areas in China and Korea prior to reaching the Baengyeong site. We plotted the natural log ( $\log_e$ ) of hourly PAN mixing ratios in ppbv against the theoretical quantiles for each season, as shown in Fig. 3. The linearity of the distribution plot indicates the log-normal distribution (Q–Q plot) pattern. In the figure, we see that PAN mixing ratios in each season followed the log-normal distribution reasonably well. However, the clear deviations from linearity at high quantiles (around 2) in summer and winter indicate abnormal behaviors of PAN at very high mixing ratios. These high-PAN spikes in summer and winter were unusual events with regard to the regional background from a purely statistical point of view. In case of relatively short-term measurements such as this study, median values were more representative for each season due to outliers on the high ends, especially in summer and winter.

The slopes of the log-normal distribution plot represent the magnitude of variance in the PAN mixing ratios. Although overall PAN mixing ratios were the lowest in summer, the variance in summer PAN mixing ratios was the greatest. The simultaneous active photochemical production and thermal destruction of PAN

**Table 1**  
Summary of observed species in each season and over entire campaign.

| Species                             | Summer |        | Autumn |        | Winter |        | Spring |        | All campaign |        |
|-------------------------------------|--------|--------|--------|--------|--------|--------|--------|--------|--------------|--------|
|                                     | Mean   | Median | Mean   | Median | Mean   | Median | Mean   | Median | Mean         | Median |
| PAN                                 | 0.068  | 0.040  | 0.72   | 0.58   | 0.38   | 0.32   | 0.22   | 0.17   | 0.38         | 0.28   |
| O <sub>3</sub>                      | 32     | 31     | 41     | 40     | 28     | 28     | 43     | 42     | 37           | 34     |
| NO <sub>x</sub>                     | 1.71   | 1.20   | 2.91   | 2.36   | 1.21   | 0.62   | 3.80   | 3.14   | 2.49         | 1.83   |
| NO <sub>y</sub>                     | 1.77   | 1.34   | 5.28   | 3.65   | 3.25   | 1.62   | 6.43   | 5.57   | 4.40         | 2.73   |
| CO                                  | 175    | 166    | 212    | 182    | 308    | 257    | 353    | 292    | 269          | 226    |
| SO <sub>2</sub>                     | 1.99   | 2.00   | 3.94   | 3.55   | 5.85   | 4.40   | 3.78   | 2.84   | 4.05         | 3.22   |
| PM <sub>2.5</sub> *                 | 14     | 12     | 14     | 12     | 13     | 10     | 26     | 22     | 17           | 13     |
| TVOC **                             | 229    | 210    | 149    | 118    | 53     | 43     | 85     | 77     | 126          | 91     |
| EC *                                | 0.65   | 0.65   | 0.68   | 0.68   | 0.32   | 0.23   | 0.93   | 0.82   | 0.65         | 0.58   |
| OC *                                | 1.79   | 1.71   | 2.34   | 1.94   | 1.68   | 0.32   | 4.35   | 4.18   | 2.57         | 1.99   |
| NO <sub>3</sub> *                   | 0.47   | 0.30   | 1.45   | 0.52   | 0.98   | 0.50   | 6.43   | 2.46   | 2.26         | 0.61   |
| nss SO <sub>4</sub> <sup>2-</sup> * | 5.58   | 3.65   | 4.94   | 4.21   | 3.19   | 3.01   | 10.8   | 9.30   | 5.79         | 4.13   |
| Temp ***                            | 24.8   | 24.9   | 15.6   | 15.5   | 0.7    | -5.6   | 6.5    | 6.1    | 10.9         | 12.8   |

All concentrations are in ppbv unless otherwise noted.

\* $\mu\text{g m}^{-3}$ , \*\*: ppbC, \*\*\*: °C.

during summer might explain the large concentration variation. Photochemical production of O<sub>3</sub> and PAN is most active during the summer if the precursors remain at constant levels. However, slow-moving summer monsoon depressions bring clean marine air to East Asia. PAN, CO and NO<sub>y</sub> remained at their lowest levels at the measurement site in the summer. In contrast to the other precursors, total VOC (TVOC) peaked in summer. It is well documented that VOCs concentrations in urban areas in Korea are lowest in summer (Na and Kim, 2001). Contrary to this fact, TVOCs in our study area were highest in summer. Especially, isopentane, toluene, ethylbenzene, and xylene (denoted as TEX) had the largest portion (57%) and isoprene was the second (11%) in summer TVOCs. These five species accounts for about 70% in summer TVOCs in measurement site. Isopentane and TEX are the representative compounds of gasoline evaporation and solvent use, respectively. Their concentrations are known to be elevated during summertime in Korea (Na and Kim, 2001). One of the largest oil refineries and petrochemical complex which are the potential sources of

isopentane and TEX is located 200 km southeast of measurement site. Based on very low concentrations of other precursors, it is likely that petrochemical emission sources by prevailing south winds and high temperature were the main causes of unusually high summertime TVOCs in this remote site. Thus, the drop in PAN in summer can be attributed to the limited availability of reactive nitrogen species and rapid thermal destruction.

In contrast to summer, the variance in PAN mixing ratios in winter was the smallest. The reduced photochemical production rate and thermal stability of PAN at low temperatures ensured a relatively narrow range of PAN levels. Although the slopes of the autumn and spring PAN Q–Q plots were similar to each other, the PAN mixing ratios in autumn were three times higher than in spring. All measured species, except PAN and TVOC, were higher in spring than autumn and the secondary species such as O<sub>3</sub> and aerosol nitrate and sulfate were also higher in spring (Table 1). For O<sub>3</sub>, its maximum in spring is consistent with other studies at regional remote sites (Monks, 2000; Salisbury et al., 2002; Sikder

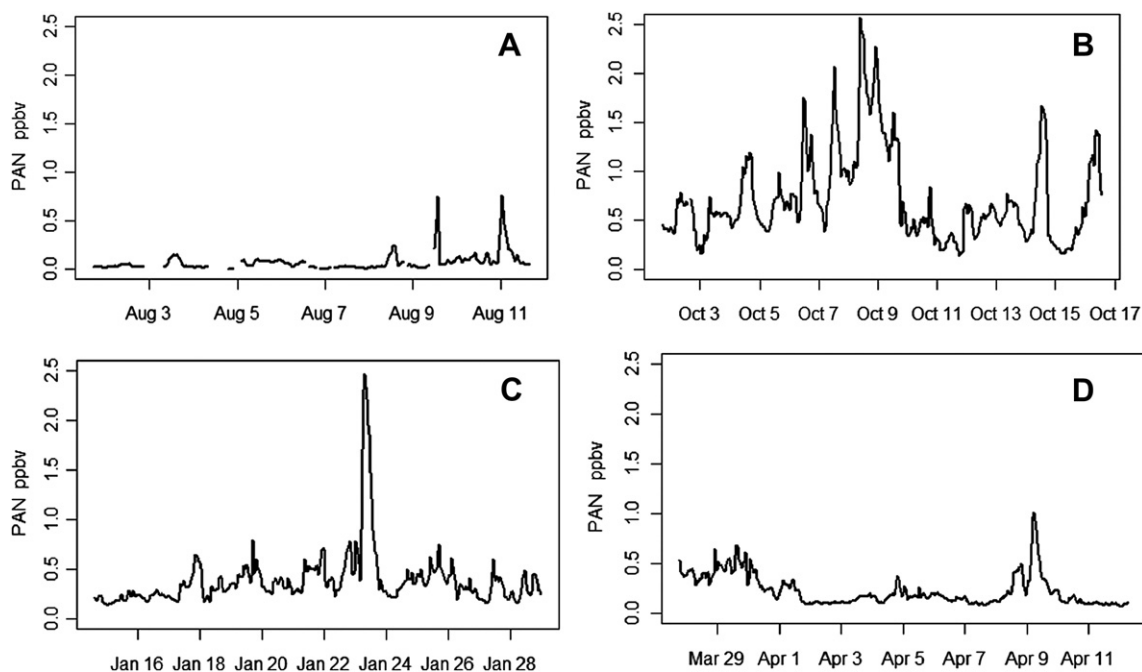


**Fig. 2.** Observed hourly PAN mixing ratios on Baeyeong Island during the four different seasons: 2010 summer (A), 2010 autumn (B), 2011 winter (C), and 2011 spring (D).

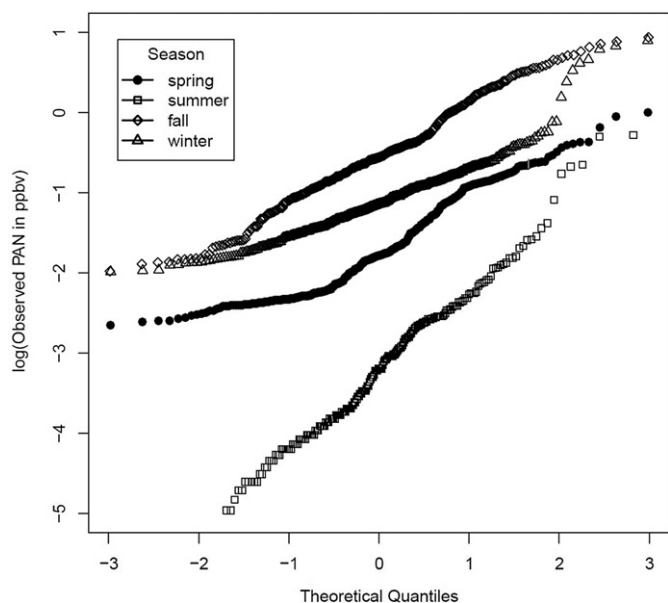


**Fig. 3.** Log-normal distributions (Q–Q plot) of hourly PAN mixing ratios in each season in 2010 and 2011.

et al., 2011; Wang et al., 2011). A seasonal pattern with a PAN maximum in autumn and  $O_3$  maximum in spring was also found in an urban area—Santiago, Chile (Rubio et al., 2007). The increased levels of precursors, associated with the stability of the atmosphere, and the decreased rate of thermal decomposition were the main causes for the maximum PAN in autumn. On Baengyeong Island, the difference in prevailing transport patterns might be the main

cause for the disparity in PAN mean concentrations between autumn and spring. In contrast to autumn, when air masses transported from the Korean peninsula were frequently observed at the measurements site, the air reaching the site had passed over inland China in spring. The air mass from China in spring had relatively low TVOC but high levels of other precursors and aerosol species. Apparently, the low TVOC level with a mean of 85 ppbC in spring was the limiting factor for PAN production on Baengyeong Island.

As seen in Fig. 4, distinct diurnal variations in PAN concentrations with an afternoon peak are most visible during the summer and autumn. This indicates that in-situ photochemical production of PAN occurs on Baengyeong Island during these seasons. In-situ production (several hundred pptv) of PAN during the autumn daytime was an important source supporting the high PAN mixing ratios in the boundary layer over the Yellow Sea. It is known that long-range transport of PAN away from source regions usually occurs in the free troposphere, where the temperature is low enough to minimize thermal decomposition and removal by deposition (Wolfe et al., 2007; Parker et al., 2009). However, our observations show that transport over considerable distances is possible by the cycling of in-situ production and thermal dissociation within the boundary layer.

Due to predominant influences from the relatively clean, slow-moving marine air masses and high temperature during the summer season, the PAN mixing ratios were mostly low with an hourly average of 0.09 ppbv, barring a few transient cases of elevated levels due to the influence of the nearby land masses. Daytime photochemical production of PAN in the summer was clearly impeded due to the limited availability of precursors despite the strong sunlight. Nearly all the PAN produced photochemically by noon was destructed within 2–3 h in the early afternoon. During

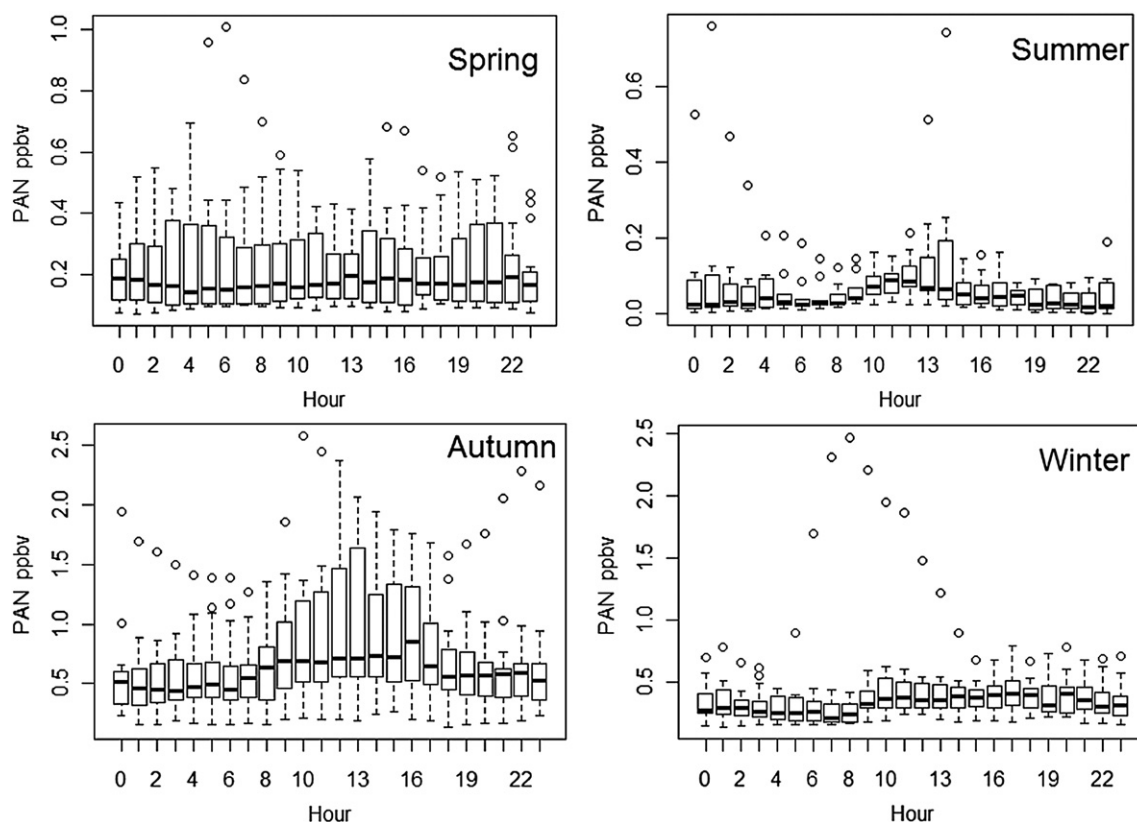


**Fig. 4.** Diurnal variations in PAN for each season. Boxes and bars represent 25–75 percentiles and 5–96 percentiles, respectively. Lines inside the boxes denote medians.

the winter and spring, photochemical production of PAN was also restricted due to limited precursor species and low sunlight intensity. The high PAN events with very short time periods (less than half day) were quite common except during daytime in all seasons (Fig. 4). These bursts of high PAN corresponded with the arrival of fast moving air masses influenced by the major emission sources in China and Korea.

### 3.2. Transportation of PAN

The most frequent and prevailing winds at the Baengyeong site were from the northwest, and usually brought continental air across the Yellow Sea (Fig. 5A). Southerly winds were also rather common during the summer and usually carried the cleanest marine air to the site. During the summer and fall, air masses that had passed over Korea were often brought over by the southeasterly winds. A PAN polar plot calculated with nonparametric K-mean regression showed that the largest mixing ratios occurred in the fast moving northwesterly winds, reflecting transport from northeastern China, especially the Beijing area (Fig. 5B). Significant  $\text{NO}_y$  was brought by the fast moving westerly winds; the closest land mass in that direction is Shandong province in inland China, which is the second most populated and industrialized area (Fig. 5C). Increased levels of  $\text{NO}_y$  were observed as well in the

moderate south and southeast winds, where the anthropogenic influences from South Korea would be dominant. A TVOC wind-rose plot showed that southeast was the upwind direction along which potential sources were located (Fig. 5D). As discussed earlier, high TVOC levels were observed during the summer. Thus, it can be inferred that the prominent sources for TVOC are anthropogenic emissions from South Korea and natural emissions from local summer vegetation, where cover extensive areas toward the southeast from the site. Despite the very high TVOC in the southeast winds, the PAN mixing ratios were low given that they had the lowest levels of  $\text{NO}_y$  and the high temperature in the summer. The wind-rose plots suggest that PAN was more closely dependent on the winds from the northwest, which had high levels of reactive nitrogen ( $\text{NO}_y$ ).

The sampling site faces the coastal areas of North Korea along the North to the East. The winds were seldom blowing from these directions. Even though the measurement site and Baengyeong Island are situated under a coastal boundary layer 10 km away from coast of North Korea, no oscillation in wind direction with land sea breezes was noticeable for all seasons. In addition to low occurrences of winds from the North to the East, the levels of PAN and its precursors were the lowest within these wind directions. Thus, it appears that North Korea does not play an important role in emissions of atmospheric pollutants over this

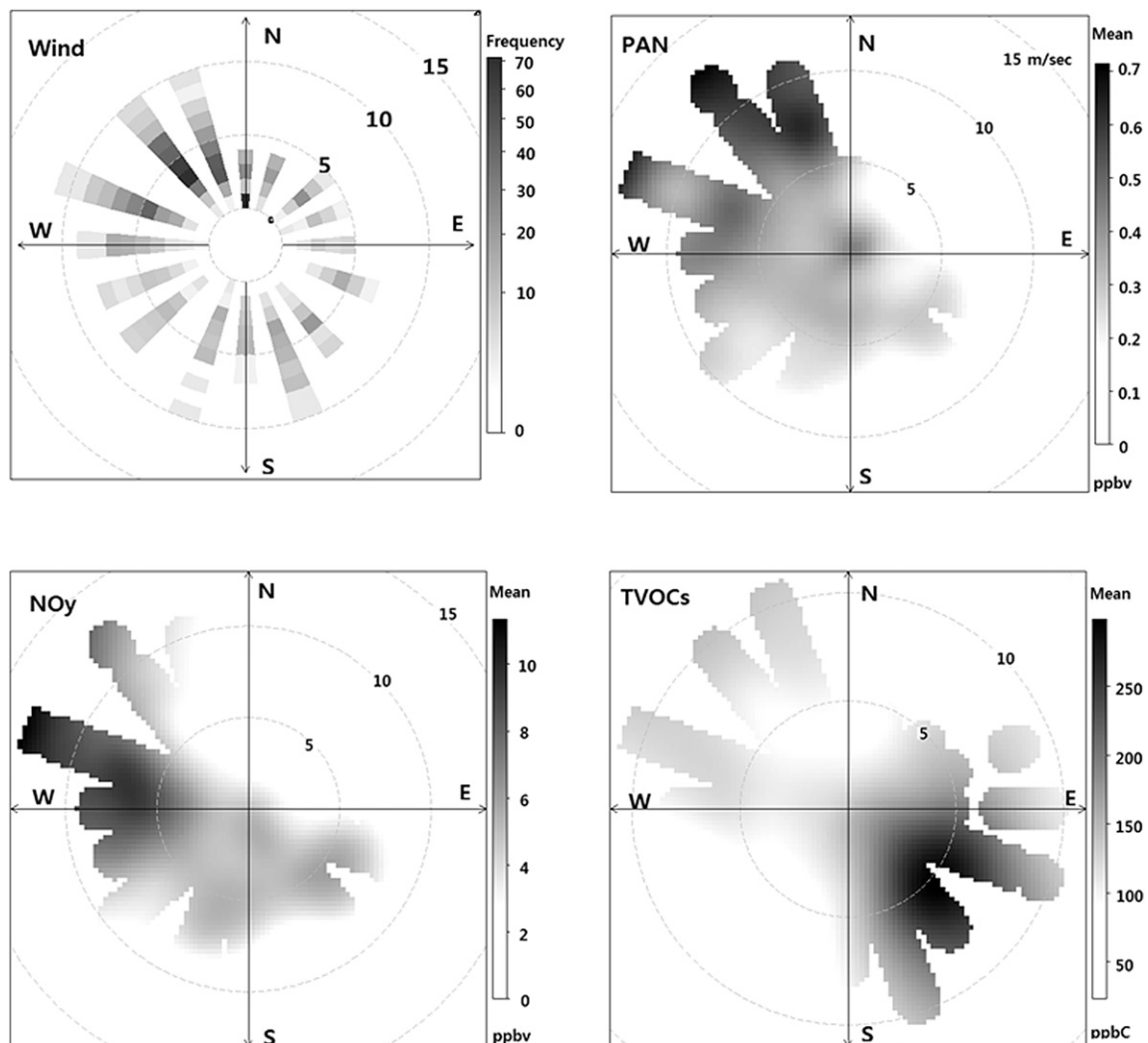


Fig. 5. Polar plots for winds, PAN,  $\text{NO}_y$ , and TVOCs using nonparametric smoothing for all season data.

region. The synoptic wind patterns and prevailing wind systems (mid-latitude westerly) from China and South Korea are the key features determining the levels of PAN measured at the Baengyeong site.

Compared with the other seasons, more regular cases of enhanced PAN were observed throughout the autumn campaign. Hence, we focus on the autumn episodes: We could classify four distinct periods (LO, SK, BC, and DC) on the basis of the behaviors of measured chemical species and back trajectories during the autumn measurement campaign (Fig. 6). The locally influenced period (LO) was characterized by high TVOC and  $\text{NO}_2$  concentrations but depleted  $\text{O}_3$ . Although the concentrations of the PAN precursors were greatly enhanced, the concentration of PAN itself was raised just slightly due to the moderate amount of precipitation in this period.

The transported air masses (SK) from industrial areas in South Korea showed the largest PAN concentrations of up to 2.6 ppbv. TVOC and nitrate aerosol concentrations were significantly enhanced compared with the other species. Moreover, the  $\text{O}_3$  concentrations reached their highest levels in this period. The air masses from the Beijing area (BC) also showed a similar pattern to that seen in the SK period, with slightly low concentrations for most species except sulfate aerosol, EC, and atmospheric aerosol lead (Pb). While most gaseous and aerosol species demonstrated

similar ranges of concentrations between the BC and DC periods,  $\text{NO}_2$  was considerably increased during the latter. Comparing with the Beijing region (BC), the short distance to the sampling site from emission sources in Liaoning province (DC) was the likely reason for the high concentrations of short-lived  $\text{NO}_2$ . It was found that air masses from Chinese (BC and DC) were typically characterized by very high concentrations of aerosol species such as sulfate aerosol, Pb, and EC, although the photochemical products  $\text{O}_3$  and PAN remained at moderate levels.

All precursors showed some degree of correlation with PAN. Especially, PAN was very well correlated with  $\text{NO}_2$  in South Korea and Beijing air mass and their slope (PAN/ $\text{NO}_2$  ratio) were close to 1. The PAN/ $\text{NO}_x$  ratio versus the  $\text{NO}_x$  mixing ratio is often used as an indicator of the air mass age (Singh et al., 1985). Higher ratios at low  $\text{NO}_x$  conditions can be expected with increasing age and photochemical decoupling of PAN and  $\text{NO}_x$ , in areas far from emission source regions. PAN/ $\text{NO}_x$  ratio of about 5 is typical of isolated maritime free tropospheric air masses with an age of 1 week (Ridley et al., 1990). PAN/ $\text{NO}_x$  ratios on Baengyeong Island were lower than those on well aged air mass. However, they were similar to those at the regional background sites in Japan (Watanabe et al., 1998). Thus, although caution should be applied in regarding Baengyeong Island as a marine remote site, it is an ideal site to monitor outflows influenced by surrounding regional anthropogenic sources.

The ratios of daily maximum PAN to  $\text{O}_3$  in daytime during autumn were in the range 0.03–0.04, with no noticeable differences between Chinese and South Korean air masses. Even though this range is similar to the value of 0.02 reported in other urban studies conducted elsewhere, it is considerably lower than the value of 0.07 measured in the Seoul Metropolitan area in South Korea in summer (Lee et al., 2008) and 0.09 at a suburban site in China (Zhang et al., 2009). The low photochemical production, thermal decomposition of PAN, and additional  $\text{O}_3$  not involved in the photochemical reaction during air mass transport are the likely causes for the reduced PAN/ $\text{O}_3$  ratio at the site compared with those in surrounding source regions.

We calculated the isentropic back trajectories using the NOAA HYSPLIT model to determine air mass positions 24 h prior reaching a height of 500 m over the Baengyeong site (Draxler and Rolph, 2012), as shown in Fig. 7. High PAN mixing ratios were mainly observed in the air masses with prior sinking motions within 2000 m above sea level. PAN mixing ratios in air masses transported at low altitudes below 500 m were clearly lower than those at higher altitudes. This suggests that the transport of PAN is more efficient at high altitude due to the fast moving air masses and relatively low temperatures, both of which ensured transport over large distances. It also indicates that the marine boundary layer acted as an overall sink for PAN, although in-situ photochemical PAN production was apparent under some conditions. We may expect higher PAN levels as the altitude increases if the removal of PAN dominates in the boundary layer. However, we found a vertical distribution of PAN with a maximum near a height of 2 km. The fast sinking air at the measurement site from altitudes higher than 2 km were did not tend to bring air from regions in close proximity to the source regions in China and Korea. The vertical trend of PAN with a mid-altitude maximum observed here is consistent with those observed in the marine atmospheres in southern Yellow Sea and near Japan during aircraft campaigns (Watanabe et al., 1998). In general, the surface PAN concentration recorded in this study was about two times higher than that of previous studies in the early 1990s. The closeness to major source regions and anthropogenic emission increase of precursors over the last two decades are likely causes for the increased surface PAN concentrations at Baengyeong Island.

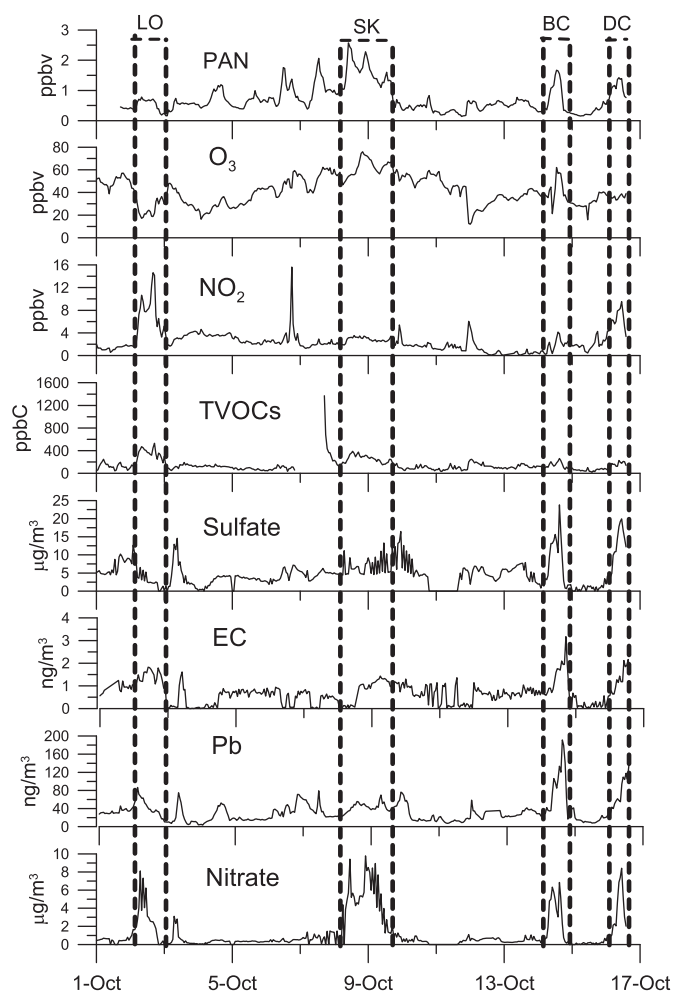


**Fig. 6.** Variations in PAN and selected gaseous and aerosol species during 2011 autumn campaign. LO, SK, BC, and DC denote the periods dominated by local sources, South Korea, the Beijing area, and the Dailan area in Liaoning province, China, respectively.

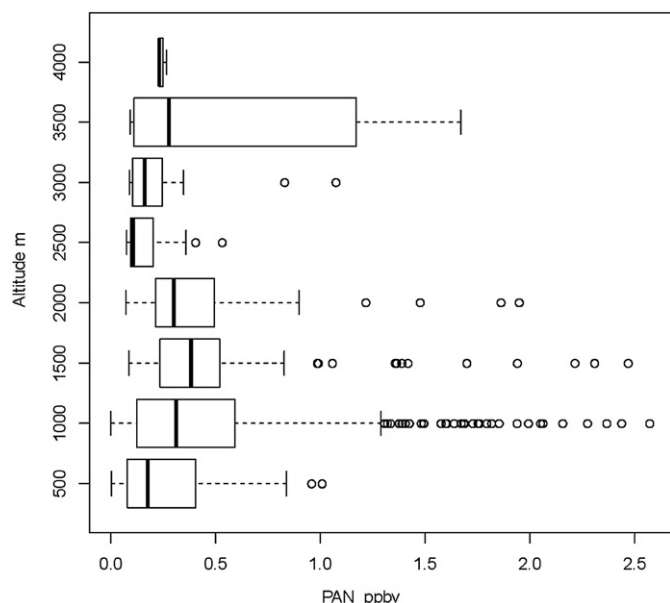


Fig. 7. Distributions of PAN mixing ratios versus altitudes of the air masses 24 h prior to arrival at Baengyeong Island. Boxes and bars represent 25–75 percentiles and 5–96 percentiles, respectively. Lines inside the boxes denote medians.

#### 4. Conclusions

We measured the mixing ratios of PAN and other major atmospheric pollutants and ionic species on Baengyeong Island in the four different seasons in 2010 and 2011. The observed PAN mixing ratio was significantly higher in October (median: 0.58 ppbv) than in summer (0.04 ppbv). Despite the intense sunlight available in summer, the prevalence of slow-moving, high-temperature clean marine air masses favored low PAN mixing ratios. The air masses originating from high altitudes prior to reaching Baengyeong Island brought in relatively high levels of PAN, which confirmed that the high-altitude outflows from the continents are efficient transport pathways that can carry PAN over extensive distances. Further, this indicates that the marine boundary layer acted as an overall sink for PAN. However, we found that in-situ photochemical PAN production was apparent under some conditions. The observed systematic daytime increase (several hundred pptv) in PAN in autumn implied that the in-situ photochemical production of insoluble PAN is an important source for maintaining high PAN mixing ratios in the boundary layer over the Yellow Sea. In addition, it might play significant role in the regional transport of reactive nitrogen species within the marine boundary layer. The photochemical ages determined from the PAN/NO<sub>x</sub> ratios indicated that the measurement site mostly represented the relatively clean regional marine boundary layer, with abrupt increases in PAN levels due to transport from the nearby land masses. Thus, PAN observations on Baengyeong Island offered an interesting chance to monitor the regional anthropogenic influence from the nearby land masses, mainly China and South Korea. However, the long-term systematic measurements of PAN and its precursors on this site are required to elucidate a more complete picture of its chemistry and transport over this region.

#### Acknowledgment

This work was supported by a Grant from the National Research Foundation of Korea (NRF-2010-0010773).

#### References

- Akimoto, H., 2003. Global air quality and pollution. *Science* 302, 1716–1719.
- Cape, J.N., 2003. Effects of airborne volatile organic compounds on plants. *Environ. Pollut.* 122, 145–157.
- Crutzen, P.J., 1979. The role of NO and NO<sub>2</sub> in the chemistry of the troposphere and stratosphere. *Annu. Rev. Earth Planet. Sci.* 7, 443–472.
- Draxler, R.R., Rolph, G.D., 2012. HYSPLIT (HYbrid Single-Particle Lagrangian Integrated Trajectory) Model Access via NOAA ARL READY. NOAA Air Resources Laboratory, Silver Spring, MD. Website: <http://ready.arl.noaa.gov/HYSPLIT.php>.
- Gaffney, J.S., Marley, N.A., 1993. Measurements of peroxyacetyl nitrate at a remote site in the southwestern United States: tropospheric implications. *Environ. Sci. Technol.* 27, 1905–1910.
- Gaffney, J.S., Fajer, R., Senum, G.I., 1984. An improved procedure for high purity gaseous peroxyacetyl nitrate production: use of heavy lipid solvents. *Atmos. Environ.* 18, 215–218.
- Gallagher, M.S., Carsey, T.P., Farmer, M.L., 1990. Peroxyacetyl nitrate in the North Atlantic marine boundary layer. *Global Biogeochem. Cycles* 4 (3), 297–308.
- Gregory, G.L., Hoell, J.M., Ridley, B.A., Singh, H.B., Gandrud, B., Salas, L.J., Shetter, J., 1990. An intercomparison of airborne PAN measurements. *J. Geophys. Res.* 95, 10077–10087.
- Hudman, R.C., Jacob, D.J., Cooper, O.R., Evans, M.J., Heald, C.L., Park, R.J., Fehsenfeld, F., Flocke, F., Holloway, J., Hübler, G., Kita, K., Koike, M., Kondo, Y., Neuman, A., Nowak, J., Oltmans, S., Parrish, D., Roberts, J.M., Ryerson, T., 2004. Ozone production in transpacific Asian pollution plumes and implications for ozone air quality in California. *J. Geophys. Res.* 109, D23S10. <http://dx.doi.org/10.1029/2004JD004974>.
- Kourtidis, K.A., Fabian, P., Zerefos, C., Rappengluck, B., 1993. Peroxyacetyl nitrate (PAN), peroxypropionyl nitrate (PPN) and PAN/ozon ratio measurements at three sites in Germany. *Tellus* 45B, 442–457.
- Lee, G.W., Jang, Y.E., Lee, H.Y., Han, J.S., Kim, K.R., Lee, M.H., 2008. Characteristic behavior of peroxyacetyl nitrate (PAN) in Seoul megacity, Korea. *Chemosphere* 73, 619–628.
- Marley, N.A., Gaffney, J.S., White, R.V., Rodriguez-Cuadra, L., Herndon, S.E., Dunlea, E., Volkamer, R.M., Molina, L.T., Molina, M.J., 2004. Fast gas chromatography with luminol chemiluminescence detection for the simultaneous determination of nitrogen dioxide and peroxyacetyl nitrate in the atmosphere. *Rev. Sci. Instrum.* 75, 4595–4605.
- Mills, G.P., Sturges, W.T., Salmon, R.A., Bauguitte, S.J.-B., Read, K.A., Bandy, B.J., 2007. Seasonal variation of peroxyacetyl nitrate (PAN) in coastal Antarctica measured with a new instrument for the detection of sub-part per trillion mixing ratios of PAN. *Atmos. Chem. Phys.* 7, 4589–4599.
- Monks, P.S., 2000. A review of the observations and origins of the spring ozone maximum. *Atmos. Environ.* 34, 3545–3561.
- Muller, K.P., Rudolph, J., 1992. Measurements of peroxyacetyl nitrate in the marine boundary layer over the Atlantic. *J. Atmos. Chem.* 15, 361–367.
- Na, K., Kim, Y.P., 2001. Seasonal characteristics of ambient volatile organic compounds in Seoul, Korea. *Atmos. Environ.* 35, 2603–2614.
- Nielsen, T., Samuelsson, U., Grennfelt, C., Thomsen, E.L., 1981. Peroxyacetyl nitrate in long-range transported polluted air. *Nature* 293, 553–555.
- Ohara, T., Akimoto, H., Kurokawa, J., Horii, N., Yamaji, K., Yan, X., Hayasaka, T., 2007. Asian emission inventory for anthropogenic mission sources during the period 1980–2020. *Atmos. Chem. Phys.* 7, 4419–4444.
- Parker, A.E., Monks, P.S., Wyche, K.P., Balzani-Lööv, J.M., Staehelin, J., Reimann, S., Legreid, G., Vollmer, M.K., Steinbacher, M., 2009. Peroxy radicals in the summer free troposphere: seasonality and potential for heterogeneous loss. *Atmos. Chem. Phys.* 9, 1989–2006.
- Pochanart, P., Kato, S., Katsuno, T., Akimoto, H., 2004. Eurasian continental background and regionally polluted levels of ozone and CO observed in northeast Asia. *Atmos. Environ.* 38, 1325–1336.
- Reidmiller, D.R., Jaffe, D.A., Chand, D., Strode, S., Swartzendruber, P., Wolfe, G.M., Thornton, J.A., 2009. Interannual variability of long-range transport as seen at the Mt. Bachelor Observatory. *Atmos. Chem. Phys.* 9, 557–572.
- Ridley, B.A., Shetter, J.D., Gandrud, B.W., Salas, L.J., Singh, H.B., Carroll, M.A., Hübler, G., Albritton, D.L., Hastle, D.R., Schiff, H.I., Mackay, G.I., Karechi, R.D., Davis, D.D., Bradshaw, J.D., Rodgers, M.O., Sandholm, S.T., Torres, A.L., Condon, E.P., Gregory, G.L., Gregory, G.L., Beck, S.M., 1990. Ratios of peroxyacetyl nitrate to active nitrogen nitrogen observed during aircraft flights over the eastern Pacific Oceans and continental United States. *J. Geophys. Res.* 95 (D7), 10,179–10,192.
- Rubio, M.A., Gramsch, E., Lissi, E., Villena, G., 2007. Seasonal dependence of peroxyacetyl nitrate (PAN) concentrations in downtown Santiago, Chile. *Atmósfera* 20 (4), 319–328.
- Salisbury, G., Monks, P.S., Bauguitte, S., Bandy, B.J., Penkett, S.A., 2002. A seasonal comparison of the ozone photochemistry in clean and polluted air masses at Mace Head, Ireland. *J. Atmos. Chem.* 41, 163–187.
- Sikder, H.A., Suthawaree, J., Kato, S., Kajii, Y., 2011. Surface ozone and carbon monoxide levels observed at Oki, Japan: regional air pollution trends in East Asia. *J. Environ. Manage.* 92, 953–959.
- Singh, H.B., Salas, L.J., Ridley, B.A., Shetter, J.D., Donahue, N.M., Fehsenfeld, E.C., Fahey, D.W., Parrish, D.D., Williams, E.J., Liu, S.C., Hübler, G., Murphy, P.C., 1985. Relationship between peroxyacetyl nitrate and nitrogen oxides in the clean troposphere. *Nature* 318, 347–349.
- Singh, H.B., Brune, W.H., Crawford, J.H., Flocke, F., Jacob, D.J., 2009. Chemistry and transport of pollution over the Gulf of Mexico and the Pacific: spring 2006

- INTEX-B campaign overview and first results. *Atmos. Chem. Phys. Discuss.* 9, 363–409.
- Staehelein, J., Poberaj, C.S., 2007. Long-term tropospheric ozone trends: a critical review. In: Brönnimann, S., Luterbacher, J., Ewen, T., Diaz, H.F., Stolarski, R.S., Neu, U. (Eds.), *Advance in Global Change Research*, vol. 33. Springer, Netherlands, pp. 271–282.
- Staudt, A.C., Jacob, D.J., Ravetta, F., Logan, J.A., Bachiochi, D., Sandholm, S., Ridley, B., Singh, H.B., Talbot, B., 2003. Sources and chemistry of nitrogen oxides over the tropical Pacific. *J. Geophys. Res.* 108 (D2), 8239. <http://dx.doi.org/10.1029/2002JD002139>.
- Sun, Y., Wang, L., Wang, Y., Quan, L., Zirui, L., 2011. In situ measurements of SO<sub>2</sub>, NO<sub>x</sub>, NO<sub>y</sub>, and O<sub>3</sub> in Beijing, China during August 2008. *Sci. Total Environ.* 409, 933–940.
- Wang, Y., Zhang, Y., Hao, J., Luo, M., 2011. Seasonal and spatial variability of surface ozone over China: contributions from background and domestic pollution. *Atmos. Chem. Phys.* 11, 3511–3525.
- Watanabe, I., Nakanishi, M., Tornita, J., Hatakeyama, S., Murano, K., Mukai, H., Bandou, H., 1998. Atmospheric peroxyacyl nitrates in urban/remote sites and the lower troposphere around Japan. *Environ. Pollut.* 102, 253–261.
- Wild, O., Prather, M.J., Akimoto, H., Sundet, J.K., Isaken, I.S.A., Crawford, J.H., Davis, D.D., Avery, M.A., Kondo, Y., Satche, G.W., Sanholm, S.T., 2004. Chemical transport model ozone simulations for spring 2001 over the western Pacific: regional ozone production and its global impacts. *J. Geophys. Res.* 109. <http://dx.doi.org/10.1029/2003JD004041>
- Wolfe, G.M., Thornton, J.A., McNeill, V.F., Jaffe, D.A., Reidmiller, D., Chand, D., Smith, J., Swartzendruber, P., Flocke, F., Zheng, W., 2007. Influence of trans-Pacific pollution transport on acyl peroxy nitrate abundances and speciation at mount bachelor observatory during INTEX-B. *Atmos. Chem. Phys.* 7, 5309–5325. <http://dx.doi.org/10.5194/acp-7-5309-2007>.
- Xu, J., Zhang, Y.H., Fu, J.S., Zheng, S.Q., Wang, W., 2008. Process analysis of typical summer ozone episodes over the Beijing area. *Sci. Total Environ.* 399, 147–157.
- Zhang, J.M., Wang, T., Ding, A.J., Zhou, X.H., Xue, L.K., Poon, C.N., Wu, W.S., Gao, J., Zuo, H.C., Chen, J.M., Zhang, X.C., Fan, S.J., 2009. Continuous measurement of peroxyacetyl nitrate (PAN) in suburban and remote areas of western China. *Atmos. Environ.* 43, 228–237.
- Zhang, J.B., Xu, Z., Yang, G., Wang, B., 2011. Peroxyacetyl nitrate (PAN) and peroxypropionyl nitrate (PPN) in urban and suburban atmospheres of Beijing, China. *Atmos. Chem. Phys. Discuss.* 11, 8173–8206.